Annealing time effect on the optical properties of Zn(O,OH,S) films onto ZnO seed layer under un-vacuum ambient

Fatma Özütok[*1] and Emin Yakar[2]

Abstract

In this study, Zn (O,OH,S) films were synthesized onto ZnO seed layers by chemical bath deposition, which were annealed at 500 °C. The differences of structural, morphological and detailed optical properties of the films were investigated depending on the annealing time (between 30 min. and 90 min.). While samples of 30.min and 90 min. showed decomposed structures, sample of 60 min. showed different dimensions of nano-flower structures. Although all films had ZnO-hexagonal crystal structure, the most obvious ZnS-related peaks were observed in the sample of 90 min. Optical absorption edge was shifted at 362 nm from Uv-Vis spectroscopy. Although ZnO, $Zn(OH)_2$ vibration related peaks were so sharp, ZnS vibration peaks were so weak for all samples from FTIR. The PL intensities were differential depending on the annealing time but defect state-corresponding peaks were similar for each films.
Keywords: Zn(O,OH,S) film, ZnO seed layer, photoluminescence spectroscopy, FTIR, optical transparency

1. INTRODUCTION

Recently, $Cu(In,Ga)(S,Se)_2$ (CIGS)- solar cells are so active research topics that has been high efficiency values over 20 %, cost-cutting effects in the industrial production and an alternative material for traditional Si-solar cells [1,3]. (CIGS)- solar cells have a layer that called as 'buffer layer' which has a relatively critical precaution for reducing the interface recombinations, decreasing the mechanical tension stress between absorbent layer/TCO electrode and providing optimal band alignment throughout the junction. CdS film preferred as a buffer layer between i:ZnO window and CIGS absorbent is produced by frequently atomic layer deposition (ALD) or chemical bath deposition (CBD) [4,5]. In the buffer layer studies, cadmium-free alternative material necessity occurs due to CdS has high toxicity, the narrow band gap energy (~2.4 eV) and high interface recombinations between the absorber and window interface [6].

Zn-component materials (ZnO, ZnS and ZnSe etc.) and their mixing materials are preferred as cadmium free alternative materials which have minimum environmentally harmful components, low optical absorption values and abundant in nature [7]. Specific amount of hydroxyl groups and impurity containing Zn(O,OH,S) film are so attractive due to their prior and tuning properties compared to other Zn-constituent materials such as large band gap energy (E_g ~2.6-3.8 eV), reduce to photocurrent loss in the short-wavelength region, high optical transparency in the UV-Vis area (>75 %) and quantum efficiency enhancing in the blue wavelength region [8].

Much more studies have been reported in the literature about ZnO- and ZnS- films which have been produced by chemical bath, spin coating, ultrasonic spray pyrolysis, atomic layer deposition (ALD) or chemical vapor deposition (CVD) [9,11]. Among them, chemical bath deposition has beneficial properties such as simple set-up, short time of chemical reactions, non-expensive, non-vacuum ambient and producible even at low temperatures (<100 °C) [12]. On the other hand,

---
* Corresponding author
[1] Çanakkale Onsekiz Mart University, Science Faculty, Physics Department, fatmaozutok@comu.edu.tr
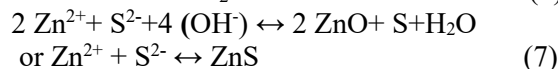[2] Çanakkale Onsekiz Mart University, Engineering Faculty, Materials Science and Engineering Department
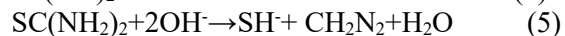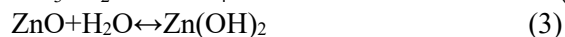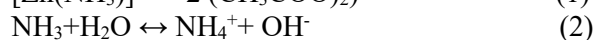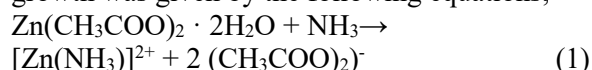
keeping under control of film growth and adherent/homogenous film production are necessary to increase buffer layer efficiency.

In this study, Zn(O,OH,S) films were synthesized onto ZnO seed layer by modified chemical bath deposition and annealing temperature was optimized at 500 °C. Using of ZnO seed layer can reduce the lattice mismatch between growing layer and substrate. Additionally, annealing time is a key parameter for improving the crystallinity and removing adsorbed impurities on the surface. Therefore, surface modification is ensured and adherent films are obtained. Structural and optical properties and surface morphology of Zn(O,OH,S) films were investigated depending on the three annealing times, 30 min., 60 min. and 90 min.

2. EXPERIMENTAL

Chemical bath deposition (CBD) technique was used for the synthesis of ZnO seed layer and Zn(O,OH,S) films. All reagents were of analytical grade and used without further purification. Amorphous glass cleaning procedure (ethanol, acetone and distilled water, respectively) was applied. ZnO seed layer preparation and ZnO film growth details were reported with modified chemical bath in our previous study [13]. In the 100 ml. distilled water including sulfide bath, 0.1 M thiourea and 0.1 M zinc-acetate dihydratre were used as S-source and Zn-source, respectively. This yellow-colored solution was mixed in an ultrasonic bath at 60±5 °C. ZnO seed layers were immersed into mixing solution while enough ammonia was dropped and optimum dipping time was determined as 4 minutes. After the film deposition, all films dried at room temperature and then annealed at 500 °C. Annealing times were chosen as 30 min., 60 min. and 90 min., respectively.

The possible chemical reactions of Zn(O,OH,S) film growth was given by the following equations;

$$Zn(CH_3COO)_2 \cdot 2H_2O + NH_3 \rightarrow$$
$$[Zn(NH_3)]^{2+} + 2 (CH_3COO)_2)^- \qquad (1)$$
$$NH_3 + H_2O \leftrightarrow NH_4^+ + OH^- \qquad (2)$$
$$ZnO + H_2O \leftrightarrow Zn(OH)_2 \qquad (3)$$
$$Zn(OH)_2 \leftrightarrow Zn^{2+} + 2OH^- \qquad (4)$$
$$SC(NH_2)_2 + 2OH^- \rightarrow SH^- + CH_2N_2 + H_2O \qquad (5)$$
$$SH^- + OH^- \rightarrow S^{2-} + H_2O \qquad (6)$$
$$2 Zn^{2+} + S^{2-} + 4 (OH^-) \leftrightarrow 2 ZnO + S + H_2O$$
$$or\ Zn^{2+} + S^{2-} \leftrightarrow ZnS \qquad (7)$$

In the Zn(O,OH,S) film growth process by CBD, Zn(OH)$_2$ layer and Zn(S, O) layer were presented and with removing the upper Zn(OH)$_2$ layer causes an improvement of buffer layer which investigated by Izaki [14]. Structural parameters of films were carried out by Rigaku SmartLab X-ray Diffractometer with CuK$_\alpha$ (1.5406 Å) radiation with powder method and step size was 0.0130 which was operated under 40 mA

and 45 kV. Average crystalline sizes were estimated by Debye-Scherer formulation which is given at below;
$$(D = 0.94\lambda/\beta\cos\theta) \qquad (8)$$
The surface morphologies and film composition of the samples were used by using JEOL JSM-7100 F SEM scanning electron microscopy and OXFORD Instruments X-Max EDX energy-dispersive x-ray spectroscopy, respectively which has been attached to each other. Optical properties (absorbance, transmittance, direct band gap energy) were investigated by Analytic Jena Uv-Vis spectroscopy which was recorded in the range of 300-900 nm. Direct band gap energies of the samples were calculated by Perrson model. At room temperature, photoluminescence intensities were measured by Quanta Master 400 Spectrofluorometer at 245 nm. excitation wavelength. FTIR (Fourier Transform Infrared Spectrum) measurements were performed on VERTEX 70 model spectrophotometer with an attenuated total reflectance (ATR) accessory between 400 and 4000 cm^{-1} (Bruker, Germany).

3. RESULTS AND DISCUSSION

In Fig.1., EDX analysis showed that all samples had different percentage of zinc, sulfur and oxygen related elemental peaks as expected in the selected region on the film surface. No impurity elements were detected while much more Zn-elemental peaks were observed in 60 min.-annealing samples, much more S-elemental peaks were observed in 90-min.-annealing samples. Additionally, annealing time had no effect on the oxygen elemental percentage from EDX analysis.
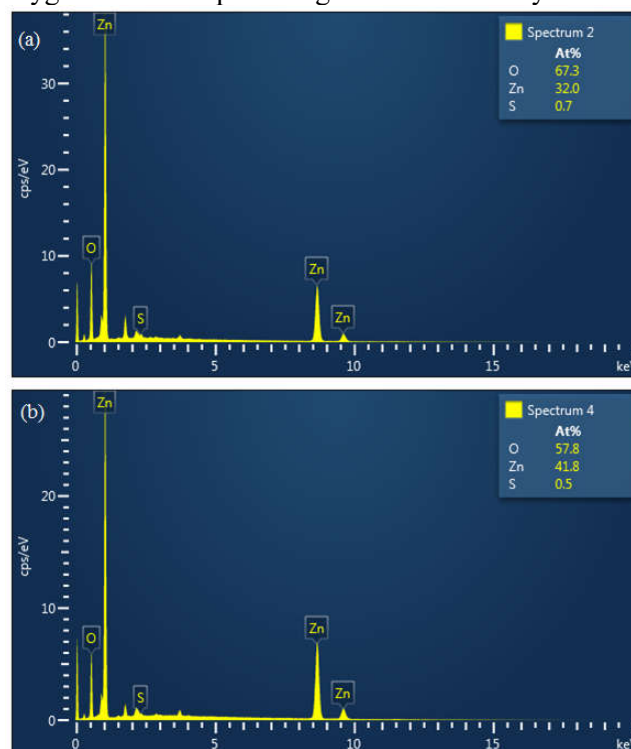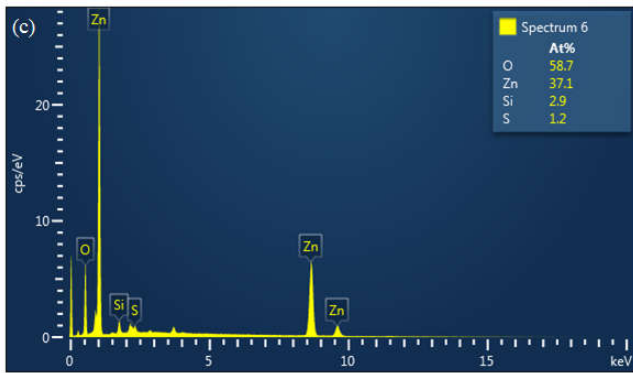
Fig.1. EDX analysis results of Zn(O,OH,S) films depending on the annealing time a)30 min. b) 60 min. and c)90 min.

The XRD profiles of samples were given in Fig.2. In the range of 2θ=20°-30°, a swelling was observed for all samples due to the amorphous glass substrate. The presence of (100), (002) and (101) peaks for all polycrystalline films represented ZnO-hexzagonal crystal structure (*JCPDS* card no:36-1451), indicating that the presence of Zn(OH)$_2$ in the range of 2θ=30°-40°. As seen in Fig. 3., all films had different XRD intensities and full width at half maximum (FWHM) depending on the annealing time. There was no ZnS-related peak detected in 30 min-and 60 min.-annealing samples. In spite of this, the most obvious ZnS-related peaks (JCPDS card no: 05-0566) were observed in sample of 90 min-annealing which indicated that enough amount S-inclusion might create weak Zn(O,S) host matrix [15]. While 30 min.-annealing samples had (100) preferential orientation, 60 min. and 90 min.-annealing samples had (101) preferential orientation. However, (002) and (101) directions for 30 min.-annealing samples and (002) and (100) directions for 60 min.- and 90 min.-annealing samples might affect the orientation. Two suggestions were given in the literature about choosing both c- and a- axis orientation. One was suggested by Mathew et.al. that high boiling points solvents cause both of orientation and (002) direction was the most thermodynamically favorable growth [16]. Another was reviewed by Znaidi et.al. that surface energy of (100) orientation was higher than (002) orientation so it was observed that (100) orientation development [17]. Having the same preferential orientation samples 60 min.- and 90 min.- annealing samples showed that intensity increased with increasing FWHM and decreasing crystallinity and also the smallest grain sizes were obtained in 60 min. annealing samples.
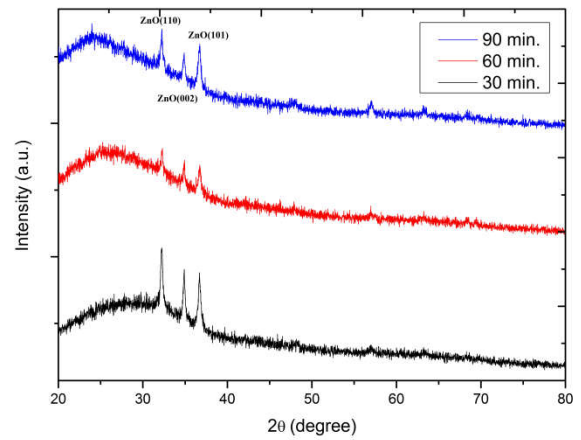

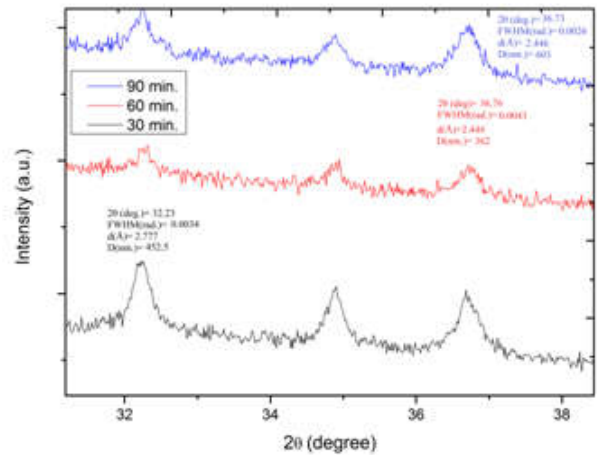Fig.2. XRD patterns of Zn(O,OH,S) films depending on the annealing time

Fig.3. Structural parameters of Zn(O,OH,S) films depending on the preferential orientation under different annealing times

The SEM cross-section image as shown in Fig.4(a). There were two different layers of micrometer level thicknesses observed which indicating layer-by-layer and Zn(O,OH,S) film which was positioned on ZnO seed layer. On the other hand Fig. 4(b), Fig 4(c) and Fig.4(d) showed that surface morphology of samples were depending on the annealing time. Nano-flower like formations and much more homogeneous surface were observed in 60 min.-annealing samples. It indicated that Zn-rich ambient created nano-flower structures which were consistent with EDX results. McPeak explained that introducing Zn into the lattice increased the CIGS buffer layer efficiency[18]. Colloidal formations were detected in 30 min. and 90 min.-annealing samples, which indicated that heterogeneous precipitation might trigger density and compactness in the film growth.
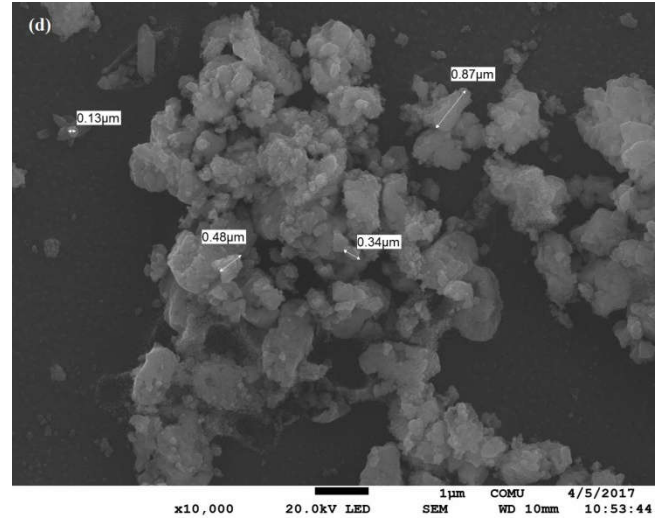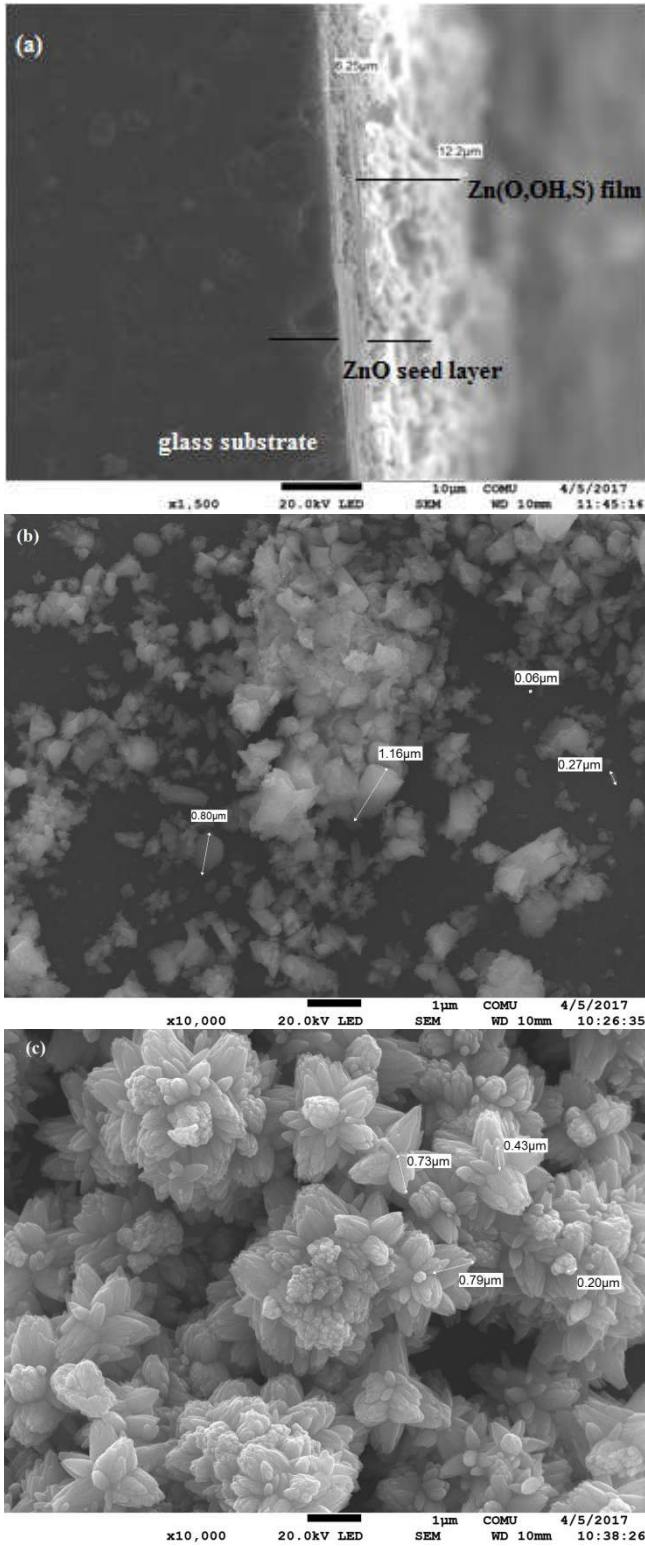
Fig.4.a)Cross section SEM image of Zn(O,OH,S) film and SEM images of Zn(O,OH,S) films for b) 30 min. c) 60 min. and d) 90 min. annealing time, respectively.

The transmission spectra of Zn(O,OH,S) films for different annealing times were shown in Fig.5. Optical absorption edge was almost coordinated at 362 nm. (3.42 eV) for all films. It was observed that red shift occured compared to ZnO seed layer (370 nm.~3.35 eV) [ref 13] due to surface kinetic processes which may affect the homogeneous film growth.

It was determined that the average value of optical transmission increased with increasing of annealing time, compatible to similar studies which was attributed to the surface impurities decreased with increasing film surface temperature[19].

A lot of band gap measurement and evolution methods have been proposed in the literature (Tauc model [20], Viezbicke fitting model [21], Kubelka–Munk function with Tauc model [22] and Kim fitting model with BM effect [23] and etc.). Among them, the equation of Perrson model [24];

$$(\alpha h\nu)=A[h\nu-E_{g,ZnO}]^{1/2}+B[h\nu-E_{g,ZnO}+\Delta E_{g}(x)]^{1/2} \quad (9)$$

was so proper for Zn(O,OH,S) films in where $\Delta E_g (x)$ was a fit parameter (x=~0.5) which varies as a function of the (S/ S+O) ratio. Band gap values were changed between 2.9±0.1 eV and 3.1±01 eV range. This band gap variation phenomenon was investigated by different research groups. Hydroxyl groups may affect the band gap values but it has been still unclear which forms in film growth [25]. A study received by Mathew that the amorphous nature of ZnO decreased as the temperature increases so the band gap energies would decrease [16]. Additionally, optical band gap changes depending on O_2 vacancies and Zn interstitial sites which given by Abdallah [26].
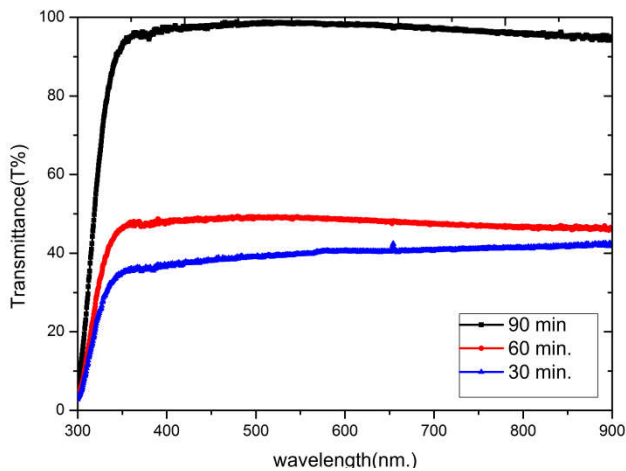
Fig.5. Optical transmittance spectrum of Zn(O,OH,S) films depending on the annealing time

FTIR spectrum gives a characteristic behavior about the vibration of atoms/molecules in the crystal structure. As can be seen in Fig. 6. hydroxyl (O-H) group stretching and bending vibrations were not observed at 3500-3900 cm^{-1} and 1400-1757 cm^{-1} respectively [27]. Very sharp peaks were determined at 410 cm^{-1} range, 765 cm^{-1} and 900 cm^{-1} which were assigned to Zn-O, OH-Zn-OH bending and M-O-M bonding vibrations [28,29,30]. Much more weak peaks were observed at 685 cm^{-1} and 2380 cm^{-1} which were attributed to Zn-S stretching and absorption of atmospheric CO_2 by a metallic cation, respectively [31,32]. These results show that proof of Zn(O,OH,S) films present onto ZnO seed layer.
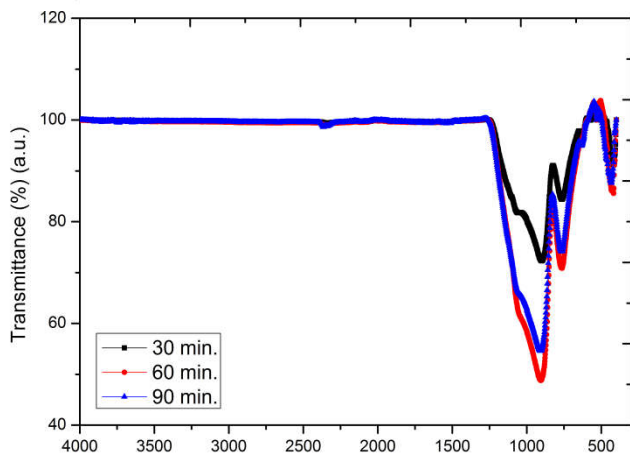

Fig.6. FTIR spectrum of Zn(O,OH,S) films depending on the annealing time

The photoluminescence (PL) spectra of Zn(O,OH,S) films were shown in Fig.7. in the range 300-650 nm. at room temperature. Detailed elemental vacancy investigation was realized by PL meausurements. As the annealing time increased, the luminescence intensity decreased between in 300-420 nm. wavelength range which indicated that decreasing density of the defects, as explained by Lu [33]. The mininum PL intensity was observed for 60-min. annealing sample which originated from Zn-rich ambient. Additionally, the PL intensities were different whereas the peak positions (defect types) were similar

for all samples as expected. Blue emission [447 nm.(2.77 eV) and 467 nm(2.65 eV)] and green emission [488 nm.(2.54 eV) and 556 nm.(2.23 eV)] were observed which can be seen in Fig.7. Generally, a blue emission was centered at between 420-450 nm. and 440-480 nm. for ZnS and ZnO films, respectively [34,35]. This ZnO type-blue emission behaviour was consistent with XRD results. Blue emission that enhanced CIGS-solar cell performance which was attributed to radiation defects relevant to interface traps on grain boundary [36]. Very strong green emission (deep level emission) was observed at 2.54 eV which wass attributed singly ionized oxygen vacancy site and its formation energy was lower than Zn_i interstitial site [37]. Another contribution to green emission came from very weak peak (2.23 eV) that would be indicating the presence of $Zn(OH)_2$. The green emission arised from that holes can recombine with electrons in the conduction band and/or shallow donor states which have been trapped at oxygen vacancies.
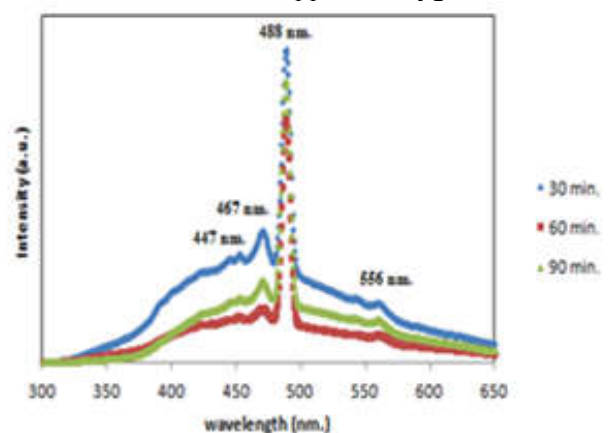

Fig.7. PL spectrum of Zn(O,OH,S) films depending on the annealing time ($\lambda_{exc.}$=245 nm.)

4. CONCLUSION

This study reported the influence annealing time on the surface morphology, crystallization, band gap energy and photoluminescence properties of chemical bath deposited Zn(O,OH,S) film onto ZnO seed layer. Annealing temperature was optimized at 500 °C and annealing times varied as 30, 60 and 90 minutes. The XRD results show that all films have ZnO-hexagonal crystal structure with different preferential orientations. Nanoflower formations were observed in 60 min.-annealing samples with minimum PL intensities. Absorption edge was coordinated at 362 nm. for all films and optical transparency decreased with increasing annealing time. FTIR spectrum was an evidence about Zn(O,OH,S) film formation. In the literature, the intensity of near band emission was varying with temperature and the increase in the deep level PL peak can cause a decrease in the diffusion length from PL spectrums of Zn(O,OH,S) films. To summarize, annealing time severely affected on the

Zn(O,OH,S) film growth thereby structural and optical properties.

REFERENCES

[1] M. Mezher, R. Garris, L. M. Mansfield, K. Horsley, L. Weinhardt, D. A. Duncan, M. Blum, S. G. Rosenberg, M. Bär, K. Ramanathan and C. Heske, "Electronic structure of the Zn(O,S)/Cu(In,Ga)Se$_2$ thin film solar cell interface", *Prog. Photovolt: Res. Appl.* Vol.24, No.8, pp.1142-1148, 2016.

[2] R. Wuerz, A. Eicke, F. Kessler, S. Paetel, S. Efimenko, C. Schlege, "CIGS thin-film solar cells and modules on enamelled steel substrates", *Solar Energy Materials & Solar Cells* Vol.100, p.p.132–137, 2012.

[3] Y.Tang, "Copper Indium Gallium Selenide Thin Film Solar Cells", *Nanostructured Solar Cells*, chapter 9, p.p.183-200, 2017.

[4] H, H, Park, R, Heasley,R. G. Gordon, "Atomic layer deposition of Zn(O,S) thin films with tunable electrical properties by oxygen annealing", *APPLIED PHYSICS LETTERS* Vol.102, No.13, p.p.132110-132115, 2013.

[5] C. Schwartz, D. Nordlund, T. Weng, D. Sokaras, L. Mansfield, A. S. Krishnapriyan, K. Ramanathan, K. E. Hurst, D. Prendergast, S. T. Christensen, "Electronic structure study of the CdS buffer layer in CIGS solar cells by X-ray absorption spectroscopy: Experiment and theory", *Solar Energy Materials & Solar Cells* Vol. 149, p.p.275–283, 2016.

[6] T. Kobayashi, Z. J. Li Kao, T. Kato, H. Sugimoto, T. Nakada, "A comparative study of Cd- and Zn-compound buffer layers on Cu(In$_{1-x}$,Ga$_x$)(S$_y$,Se$_{1-y}$)$_2$ thin film solar cells", *Prog. Photovolt: Res. Appl.* Vol.24, No.3, p.p.389–396, 2016.

[7] B. T. Ahn, L. Larina, Ki H. Kim, S. Ji Ahn, "Development of new buffer layers for Cu(In,Ga)Se$_2$ solar cells", *Pure Appl. Chem.* Vol.80, No.10, p.p. 2091–2102, 2008.

[8] C. Hubert , N. Naghavi, O. Roussel, A. Etcheberry, D. Hariskos, R. Menner, M. Powalla, O. Kerrec, D. Lincot, "The Zn(S,O,OH)/ZnMgO Buffer in Thin Film Cu(In,Ga)(S,Se)$_2$-Based Solar Cells Part I: Fast Chemical Bath Deposition of Zn(S,O,OH) Buffer Layers for Industrial Application on Co-evaporated Cu(In,Ga)Se$_2$ and Electrodeposited CuIn(S,Se)$_2$ Solar Cells", *Prog. Photovolt: Res. Appl.* Vol.17,No.7, p.p. 470–478, 2009.

[9] E.Muchuweni, T.S. Sathiaraj, H. Nyakotyo, "Synthesis and characterization of zinc oxide thin films for optoelectronic applications", *Heliyon*, Vol.3, No.4, p.p. 2405-2423, 2017.

[10] C.H. Sun, P. Zhang, T.N. Zhang, X. Chen, Y.Y. Chen, Z.H. Ye, "ZnS thin films grown by atomic layer deposition on GaAs and HgCdTe substrates at very low temperature", *Infrared Physics & Technology,* Vol.85, p.p. 280–286, 2017.

[11] F. U Hamelmann, "Thin film zinc oxide deposited by CVD and PVD", *Journal of Physics: Conference Series* Vol.764 p.012001, 2016.

[12] P.B. Taunk, R. Das, D.P. Bisen, R.K. Tamrakar, Nootan Rathor, "Synthesis and optical properties of chemical bath deposited ZnO thin film", *Karbala International Journal of Modern Science* Vol.1, No.3, p.p. 159-165, 2017.

[13] F.Özütok, S.Demiri, "Nanoflower-like ZnO Films Prepared by Modified Chemical Bath Deposition: Synthesis, Optical Properties and NO$_2$ Gas Sensing Mechanism", *Digest Journal of Nanomaterials and Biostructures* Vol.12, No.2, p.p. 309-317, 2017.

[14] M. Izaki, S. Sugiyama, T. Okamoto, Y. Kusano, T. Maki, H. Komaki, H. Shibata and S. Niki, "Structure of chemically deposited Zn(S,O,OH) buffer layer and the effects on the performance of Cu(In,Ga)Se$_2$ solar cell", *Prog. Photovolt: Res. Appl.* Vol.24, No. 3, p.p. 397–404, 2016.

[15] H ullah. A. Iqbal, M. Zakria and A. Mahmood, "Structural and spectroscopic analysis of wurtzite (ZnO)$_{1-x}$(Sb$_2$O$_3$)$_x$ composite semiconductor", *Progress in Natural Science: Materials International* Vol.25, No.2, p.p. 131–136,2015.

[16] J. P. Mathew, G. Varghese and Jacob Mathew, "Effect of post-thermal annealing on the structural and optical properties of ZnO thin films prepared from a polymer precursor", Vol.21, No.7, p.p.078104-078112, 2012.

[17] L.Znaidi, "Sol–gel-deposited ZnO thin films: A review", *Mat. Sci. Eng. B* Vol.174, No.1-3, p.p.18-30, 2010.

[18] K. M. McPeak, B. Opasanont, T. Shibata, D. Ko, M. A. Becker, S. Chattopadhyay, H. P. Bui, T. P. Beebe, Jr. Bruce A. Bunker, C. B. Murray and J. B. Baxter, "Microreactor Chemical Bath Deposition of Laterally Graded Cd1−xZnxS Thin Films: A Route to High-Throughput

Optimization for Photovoltaic Buffer Layers", *Chem.of. Mat.*, Vol. 25,No.3, p.p.297-306, 2013.

[19] V. Ghafouri, A. Ebrahimzad, M. Shariati, "The effect of annealing time and temperature on morphology and optical properties of ZnO nanostructures grown by a self-assembly method", *Scientia Iranica F* Vol.20, No.3, p.p.1039–1048, 2013.

[20] J. Tauc, R. Grigorovici, A. Vancu, "Optical properties and electronic structure of amorphous germanium", *Phys. Status Solidi* Vol.15, No. 2, p.p.627–637, 1966.

[21] B.D. Viezbicke, S. Patel, B.E. Davis and D.P. Birnie, "Evaluation of the Tauc method for optical absorption edge determination: ZnO thin films as a model system", *Phys. Status Solidi B* Vol.252 , No.8, p.p.1700- 1710, 2015.

[22] S. Ebraheem, A, El-Saied, "Band Gap Determination from Diffuse Reflectance Measurements of Irradiated Lead Borate Glass System Doped with TiO_2 by Using Diffuse Reflectance Technique", *Materials Sciences and Applications*, Vol.4, No. 5, p.p.324-329, 2013.

[23] C. E. Kim, P. Moon, S. Kim, J. Myoung, H. W. Jang, J. Bang, I. Yun, "Effect of carrier concentration on optical bandgap shift in ZnO:Ga thin films", *Thin Solid Films*, Vol.518, No. 22, p.p. 6304–6307, 2010.

[24] C.Persson, "Strong Valence-Band Offset Bowing of $ZnO_{1-x}S_x$ Enhances p-Type Nitrogen Doping of ZnO-like Alloys", *PHYSICAL REVIEW LETTERS*, Vol.97, No. 14, p.p.146403-146407, 2006.

[25] N.K. Allouche, T.B. Nasr, N.T.Kamouna and C. Guasch, "Synthesis and properties of chemical bath deposited ZnS multilayer films", *Materials Chemistry and Physics* Vol.123, p.p.620-624, 2010.

[26] B. Abdallah, A. K. Jazmatia, R. Refaai, "Oxygen Effect on Structural and Optical Properties of ZnO Thin Films Deposited by RF Magnetron Sputtering", *Materials Research*, Vol.20, No.3, p.p. 607-612, 2017.

[27] V. D. Mote, V. R. Huse, B. N. Dole, "Synthesis and Characterization of Cr Doped ZnO Nanocrystals", *World Journal of Condensed Matter Physics*, Vol.2, p.p.208-211, 2012.

[28] G. Janita Christobel, "Vibrational Spectroscopy of ZnO-ZnS Nanoparticles", *International Journal of Science and Research*, Vol.5, No. 6, p.p. 2228-2230, 2016.

[29] O. K. Srivastava, E. A. Secco, "Studies on metal hydroxy compounds: Infrared spectra of zinc derivatives Ɛ-$Zn(OH)_2$,β -ZnOHCl, ZnOHF, $Zn_5(OH)_8C_{12}$, and $Zn_6(0H),C_{12}$- H_20", *CANADIAN JOURNAL OF CHEMISTRY*, Vol.45, p.p. 585-588, 1967.

[30] W.B.White and R.Roy, "Infrared spectra-crystal structure correlatıons: comparıson of sımple polymorphıc mınerals", *THE AMERICAN MINERALOGIST*, Vol. 49, p.p.1670-1688, 1964.

[31] A. G. Rojas-Hernandez, K. J. Mendoza-Pena, E. Troyo-Vega, C. G. Perez-Hernandez, S. Munguia-Rodriguez, T. Mendıvılreynoso, L. P. Ramirez-Rodriguez, R. Ochoa-Landin, M. E. Alvarez-Ramos, A. Deleon and S. J. Castillo, "ZnS nanoparticles synthesized through chemical aggregation using polyethyleneimine that works as both a stabilizer and a complexing agent", *Chalcogenide Letters*, Vol. 14, No.1, p.p. 25-30, 2017.

[32] A. Totterdill, T. Kovács, W. Feng, S Dhomse , C. J. Smith, J. C. Gómez-Martín, M. P. Chipperfield, P. M. Forster and J. M. C. Plane, "Atmospheric lifetimes, infrared absorption spectra, radiative forcings and global warming potentials of NF_3 and CF_3CF_2Cl (CFC-115)", *Atmos. Chem. Phys.* Vol. 16, p.p.11451–11463, 2016.

[33] L.Lu, M.Wong, "The Resistivity of Zinc Oxide Under Different Annealing Configurations and Its Impact on the Leakage Characteristics of Zinc Oxide Thin-Film Transistors", *IEEE TRANSACTIONS ON ELECTRON DEVICES* , Vol.61, No. 4, p.p.1077-1084, 2014.

[34] Z. Chen, X.X. Li, D. Guoping, Q. Yu, B. Li and X. Huang, "Luminescence properties of chlorine and oxygen co-doped ZnS nanoparticles synthesized by a solid-state reaction", *Ceramics International*, Vol. 40, No.8, p.p.13151- 13157, 2014.

[35] R. Jayakrishnan, K. Mohanachandran, R. Sreekumar, C.S. Kartha and K.P. Vijayakumar, "ZnO thin films with blue emission grown using chemical spray pyrolysis", *Materials Science in Semiconductor Processing*, Vol.16, No.2, p.p.326-331, 2013.

[36] P. A. Rodnyi and I. V. Khodyuk, "Optical and Luminescence Properties of Zinc Oxide", *OPTICS AND SPECTROSCOPY* Vol.111, No. 5, p.p.776-785, 2011.

[37] Y. Gong, T. Andelman, G. F. Neumark, S. O'Brien and I. L. Kuskovsky, "Origin of defect-related green emission from ZnO nanoparticles: effect of surface modification", *Nanoscale Res Lett.*, Vol.2, p.p.297–302, 2007.